

Half-life of the $15/2^+$ state of ^{135}I : A test of $E2$ seniority relations

P. Spagnoletti,^{1,2} G. S. Simpson,^{1,2,3,*} R. Carroll,⁴ J.-M. Régis,⁵ A. Blanc,⁶ M. Jentschel,⁶ U. Köster,⁶ P. Mutti,⁶ T. Soldner,⁶ G. de France,⁷ C. A. Ur,⁸ W. Urban,⁹ A. M. Bruce,¹⁰ F. Drouet,³ L. M. Fraile,¹¹ L. P. Gaffney,^{1,2} D. G. Ghită,¹² S. Ilieva,¹³ J. Jolie,⁵ W. Korten,¹⁴ T. Kröll,¹³ C. Larijani,^{4,15} S. Lalkovski,¹⁶ R. Lică,¹² H. Mach,^{11,17} N. Mărginean,¹² V. Pazių,¹¹ Zs. Podolyák,⁴ P. H. Regan,^{4,15} M. Scheck,^{1,2} N. Saed-Samii,⁵ G. Thiamova,³ C. Townsley,⁴ A. Vancraeynest,³ V. Vedia,¹¹ A. Gargano,¹⁸ and P. Van Isacker^{7,†}

¹School of Engineering, University of the West of Scotland, Paisley PA1 2BE, United Kingdom

²Scottish Universities Physics Alliance, University of Glasgow, Glasgow G12 8QQ, United Kingdom

³LPSC, Université Joseph Fourier Grenoble 1, CNRS/IN2P3, Institut National Polytechnique de Grenoble, F-38026 Grenoble Cedex, France

⁴Department of Physics, University of Surrey, Guildford GU2 7XH, United Kingdom

⁵Institut für Kernphysik der Universität zu Köln, Zùlpicher Strasse 77, 50937 Köln, Germany

⁶Institut Laue-Langevin, 71 avenue des Martyrs, 38042 Grenoble Cedex 9, France

⁷Grand Accélérateur National d'Ions Lourds, CEA/DRF–CNRS/IN2P3, Boulevard Henri Becquerel, F-14076 Caen, France

⁸INFN, via Marzolo 8, 35131 Padova, Italy

⁹Faculty of Physics, University of Warsaw, ulica Pasteura 5, PL-02-093, Warsaw, Poland

¹⁰SCEM, University of Brighton, Lewes Road, Brighton BN2 4GJ, United Kingdom

¹¹Grupo de Física Nuclear, FAMN, Universidad Complutense, 28040 Madrid, Spain

¹²Horia Hulubei NIPNE, 77125 Bucharest, Romania

¹³Institut für Kernphysik, TU Darmstadt, Schlossgartenstrasse 9, 64289 Darmstadt, Germany

¹⁴CEA de Saclay, IRFU, 91191 Gif-sur-Yvette, France

¹⁵National Physical Laboratory, Teddington, Middlesex TW11 0LW, United Kingdom

¹⁶Faculty of Physics, University of Sofia, 1164 Sofia, Bulgaria

¹⁷National Centre for Nuclear Research, ulica Hoza 69, Warsaw, Poland

¹⁸Istituto Nazionale di Fisica Nucleare, Complesso Universitario di Monte S. Angelo, Via Cintia I-80126 Napoli, Italy

(Received 23 November 2016; revised manuscript received 20 January 2017; published 15 February 2017; corrected 22 February 2017)

The half-life of the $15/2^+$ state of the 3-valence-proton nucleus ^{135}I has been measured to be 1.74(8) ns using the EXILL-FATIMA mixed array of Ge and LaBr₃ detectors. The nuclei were produced following the cold neutron-induced fission of a ^{235}U target at the PF1B beam line of the Institut Laue-Langevin. The extracted $B(E2; 15/2^+ \rightarrow 11/2^+)$ value enabled a test of seniority relations for the first time between $E2$ transition rates. Large-scale shell-model calculations were performed for ^{134}Te and ^{135}I , and reinterpreted in a single-orbit approach. The results show that the two-body component of the $E2$ operator can be large whereas energy shifts due to the three-body component of the effective interaction are small.

DOI: [10.1103/PhysRevC.95.021302](https://doi.org/10.1103/PhysRevC.95.021302)

Detailed predictions of the structure of an atomic nucleus are nowadays routinely obtained by means of the nuclear shell model [1]. By virtue of the concept of closed shells, the description of this complex quantal system with often more than 100 interacting nucleons can be transformed into a tractable problem that considers interactions between valence nucleons only. A shell-model calculation for a medium-mass or heavy nucleus then inevitably proceeds with the choice of a truncated Hilbert space, requiring the use of effective operators tailored specifically for that space. It is by now well understood that this leads to higher-order terms in the operators, for example, to an *effective* three-body component of the nuclear interaction, not to be confused with its *genuine* three-body component [2]. While higher-order effective interactions are frequently considered, for transition operators the usual approach is to introduce effective charges at the one-body level; see, e.g., Refs. [3,4]. Only exceptionally a two-body piece is

evaluated from perturbation theory; an example is Ref. [5] where it is done for the $M1$ operator. Here we investigate the two-body part of the $E2$ operator.

As an alternative to the above numerical approach to the shell model, powerful symmetry techniques exist, leading to analytic solutions of the many-body problem in the case of specific forms of the interaction [6]. In semimagic nuclei with only one type of valence nucleon occupying a single orbit, this gives rise to a classification of nuclear states in terms of a seniority quantum number [7], which counts the number of nucleons not in pairs coupled to angular momentum $J = 0$. One particular result of the seniority scheme is that the properties of a nucleus can be written in terms of those of its neighbor with one fewer valence nucleon [8,9]. This simple approach has given rise to elegant relations between excitation spectra of neighboring nuclei but its validity has yet to be examined for other nuclear-structure properties, such as electromagnetic decay rates.

With its first-excited state above 4 MeV in energy, ^{132}Sn is arguably the most robust heavy, doubly magic nucleus. The single-valence-proton nucleus ^{133}Sb has a well-isolated

*simpson@lpsc.in2p3.fr

†isacker@ganil.fr

$7/2^+$ ground state and its first-excited level is situated at almost 1 MeV in excitation energy. The low-lying states of the respective 2- and 3-valence-proton nuclei ^{134}Te and ^{135}I are therefore comprised almost entirely of configurations involving the $\pi g_{7/2}$ orbit only [10–12] and hence provide an ideal testing ground of the seniority scheme, especially as seniority is conserved for all interactions in an orbit with $j \leq 7/2$ [8,9]. Since all $B(E2)$ values in the $6^+ \rightarrow 4^+ \rightarrow 2^+ \rightarrow 0^+$ cascade in ^{134}Te are known experimentally [10], we have a unique opportunity to apply for the first time seniority relations to electromagnetic decay rates. With this in mind we have measured the half-life of the $15/2^+$ state of ^{135}I , from which the $B(E2; 15/2^+ \rightarrow 11/2^+)$ value can be extracted. As the $\pi g_{7/2}$ orbit is isolated, the effects of other orbits can be treated in perturbation theory, enabling a transparent analysis of higher-order terms in the Hamiltonian and $E2$ operators.

The nucleus ^{135}I is situated 8 neutrons beyond the last stable iodine isotope. A limited number of reactions are available to produce this nucleus, which has mostly been studied in the past following β decay [13] or via prompt γ -ray spectroscopy of secondary fission fragments [11]. The latter reaction has been used in the present experiment to populate excited states in ^{135}I and the half-life of the $15/2^+$ state has been measured using a mixed array of Ge and $\text{LaBr}_3(\text{Ce})$ detectors. This is the first time a mixed Ge- LaBr_3 array has been used to measure half-lives of excited states in fission fragments.

The experiment was performed at the PF1B cold-neutron guide of the high-flux reactor of the Institut Laue-Langevin [14] within the framework of the EXILL-FATIMA campaign [15]. The beam was collimated down to $\sim 1 \text{ cm}^2$ in area [16] and used to induce fission in an 0.8-mg $^{235}\text{UO}_2$ (0.675-mg ^{235}U) target. The target was sandwiched between two 15- μm -thick Be backings, in order to stop the fission fragments in a time of just a few ps, minimizing the Doppler broadening of any emitted prompt γ rays. The target was then placed at the center of the EXILL-FATIMA γ -detector array, which consisted of 8 EXOGAM Clover Ge and 16 LaBr_3 detectors [15]. The data were acquired during a two-week measurement and sorted offline into $\gamma(\text{Ge})$ - $\gamma(\text{LaBr}_3)$ - $\gamma(\text{LaBr}_3)$ coincidence events, occurring within a 120-ns time window. The good energy resolution of the Ge detectors meant that gates set on their energy signals could be used to partially select the γ cascade of interest. The energy signals from the LaBr_3 detectors then provided further discrimination while their ~ 200 ps time resolution allowed the half-lives of excited states in the time range ~ 10 ps–10 ns to be measured directly. Timing signals of the LaBr_3 detectors were recorded in analog time-to-amplitude converters (TAC) with a 50-ns range. More details on the experiment can be found in Ref. [15].

The yrast $17/2^+$, $15/2^+$, $11/2^+$, and $7/2^+$ states of ^{135}I are connected by a cascade of three coincident γ decays with energies of 572.4, 288.1, and 1133.4 keV, respectively [11,12]. To verify that these transitions were not contaminated by other γ decays from any of the over 100 fission fragments produced in the reaction, $\gamma(\text{Ge})$ - $\gamma(\text{Ge})$ - $\gamma(\text{LaBr}_3)$ events were sorted. A Ge spectrum was produced by setting a gate on the 1133.4-keV γ -ray signals in the Ge detectors and the 572.4-keV transition in the LaBr_3 detectors, as shown in Fig. 1(a). Here peaks are seen from the $15/2^+ \rightarrow 11/2^+$,

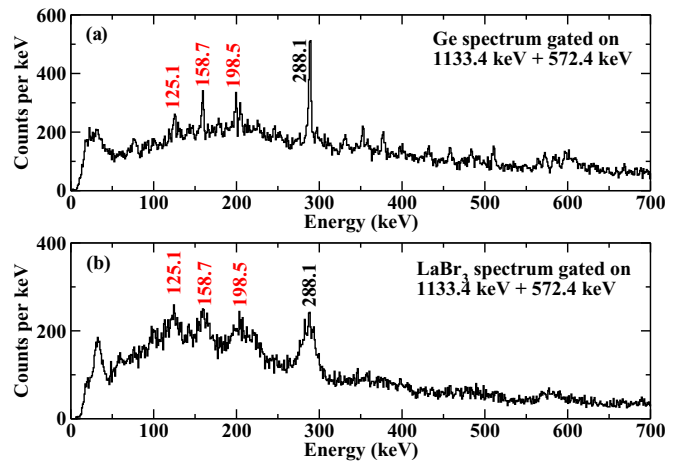


FIG. 1. (a) A Ge- $\gamma(\text{Ge})$ - $\gamma(\text{LaBr}_3)$ coincidence spectrum gated on the 572.4- and 1133.4-keV transitions of ^{135}I . (b) A LaBr_3 - $\gamma(\text{Ge})$ - $\gamma(\text{LaBr}_3)$ coincidence spectrum gated on the 1133.4- and 572.4-keV γ decays. Transitions from the most strongly produced fission-fragment partner, ^{99}Y , are indicated in red.

288.1-keV transition emitted by ^{135}I along with several others from its most likely fission-fragment partner in the $^{235}\text{U}(n,\text{F})$ reaction, ^{99}Y . The spectrum presented in Fig. 1(a) shows that the 288.1-keV γ ray is well isolated from any possible contaminant transitions and can be used as a gate in the LaBr_3 detectors to determine the half-life of the $15/2^+$ state, via a 1133.4(Ge)-572.4(LaBr_3)-288.1(LaBr_3)-keV triple coincidence.

In order to extract timing information, a gate was set on the 1133.4-keV transition in the Ge detectors and on the 572.4-keV γ decay in the LaBr_3 detectors and the events satisfying these conditions sorted into two LaBr_3 - LaBr_3 energy-time matrices. In one of these the 572.4-keV γ ray started a TAC and in the other it provided the stop signal. The projection of the energy axis of one of these matrices is shown in Fig. 1(b) and its features are identical to those of the equivalent Ge spectrum in Fig. 1(a), showing that the LaBr_3 - LaBr_3 time signals are suitable for half-life measurements to be performed. Setting gates on the 288.1-keV γ ray in the LaBr_3 - LaBr_3 energy-time matrices and subtracting an appropriate background allowed the time distribution of the 288.1-572.4-keV coincidence, and its inverse, to be obtained, as shown in Fig. 2. A clear exponential decay component is also seen on one side of each time distribution, arbitrarily centered at a time of ~ 24 ns. Fits to these slopes allow half-life values of 1.81(18) and 1.85(14) ns to be measured. One notes that the direction of both slopes confirms that the 572.4-keV transition feeds the $15/2^+$ level and the 288.1-keV one decays out of it, as placed in the level schemes of Refs. [11,12].

The half-life of the 1133.4-keV state is expected to be ~ 1 ps. Analysis of the 1133.4(LaBr_3)-572.4(LaBr_3)-288.1(Ge)-keV triple coincidences therefore allows a further independent measurement of the half-life of the 1421.5-keV, $15/2^+$ level. Values of 1.67(14) and 1.65(14) ns were determined following an analogous procedure to that described above. Combining all four measurements gives a weighted average of

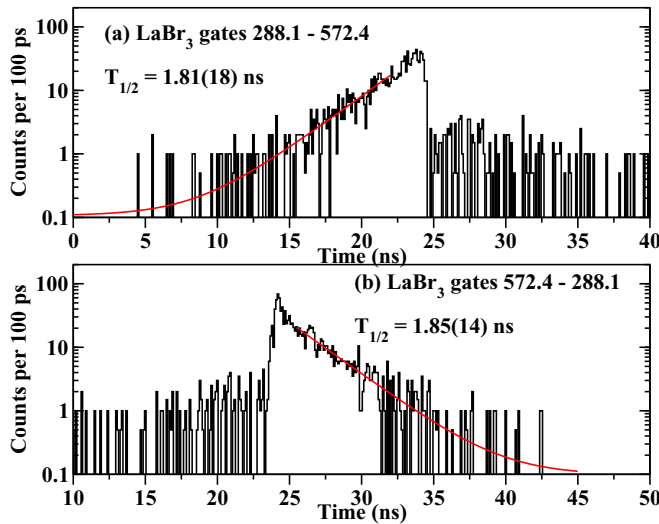


FIG. 2. Background-subtracted time spectra obtained from the LaBr_3 detectors when gated on the 1133.4- (Ge), 288.1- (LaBr_3), and 572.4-keV (LaBr_3) transitions.

$T_{1/2} = 1.74(8)$ ns for the 1421.5-keV, $15/2^+$ state of ^{135}I , which, once corrected for internal conversion ($\alpha = 0.0458$), gives $B(E2; 15/2^+ \rightarrow 11/2^+) = 3.81(17)$ W.u.

Large-scale shell-model calculations for low-lying states in the nuclei ^{134}Te and ^{135}I are reported by Goodin *et al.* [12]. These are performed using a state-of-the-art effective interaction constructed from a CD-Bonn bare nucleon-nucleon potential and renormalized following a $V_{\text{low-k}}$ approach. A ^{132}Sn closed core is employed and valence protons are allowed to occupy the $g_{7/2}$, $d_{5/2}$, $d_{3/2}$, $s_{1/2}$, and $h_{11/2}$ orbits, without further truncation. The single-particle energies are taken from the experimental spectrum of ^{133}Sb and an effective charge of $e_\pi = 1.55e$ is used. These calculations reproduce well-known energies, transition rates, and magnetic moments of states in ^{134}Te and ^{135}I [12]. In particular, the energies of all states in ^{134}Te and ^{135}I , relevant to this work, are reproduced with a precision better than 110 keV. A $B(E2; 15/2^+ \rightarrow 11/2^+) = 3.67$ W.u. is calculated, in agreement with our measured value of $3.81(17)$ W.u.

The calculated wave functions of all levels shown in Fig. 3 are dominated (more than 90%) by the $g_{7/2}^2$ and $g_{7/2}^3$ configurations in ^{134}Te and ^{135}I , respectively, with the exceptions of the ground states (80%) and the $17/2^+$ state of ^{135}I ($g_{7/2}^2 d_{5/2}^1$). This high purity is in line with the qualitative arguments presented above and allows the interpretation of properties of ^{135}I in terms of those of ^{134}Te . Seniority relations between two- and three-nucleon spectra are well known for excitation energies [8,9]. They can be extended to $E2$ properties. For example, the measured $B(E2)$ value in ^{135}I can be written as

$$B(E2; 15/2^+ \rightarrow 11/2^+) = \left(\frac{307}{242} \sqrt{\frac{B_4}{11}} + \frac{419}{231} \sqrt{\frac{2B_6}{11}} \right)^2,$$

where $B_R \equiv B(E2; R \rightarrow R - 2)$ refers to a transition in ^{134}Te . Relations of this type are applied to obtain the calculated energies and $B(E2)$ values for ^{135}I shown in Fig. 3.

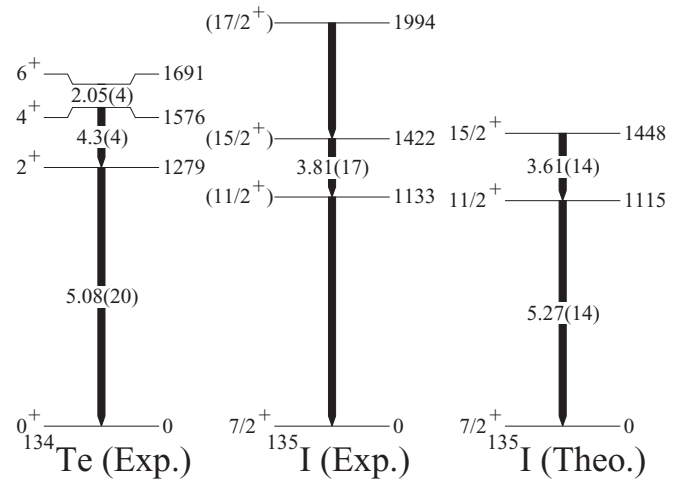


FIG. 3. Partial experimental and calculated decay schemes of ^{134}Te and ^{135}I . The theoretical values for ^{135}I are calculated from ^{134}Te , as explained in the text. $B(E2)$ values (in W.u.) are labeled on the arrows, where known or calculated.

The purity of the $g_{7/2}^2$ and $g_{7/2}^3$ configurations also allows the treatment of the other orbits in perturbation theory. The excluded orbits lead to effective operators in the single- j space that are of higher order, in particular three-body effective interactions and two-body effective transition operators [17]. In $f_{7/2}$ nuclei, effective interactions with a three-body component have been shown to occur, both in a phenomenological analysis of spectra [18] as well as in a perturbation treatment of excluded orbits of the full pf shell [19]. We perform here a similar perturbation analysis for the $g_{7/2}$ shell that is further extended to $E2$ transitions.

The relevant formulas for the effective interaction in a single $n\ell j$ shell are derived in Refs. [17,19]. Similarly, the electric-transition one-body operator $T_{1\mu}^{(\lambda)} \equiv \sum_k r_k^\lambda Y_{\lambda\mu}(\theta_k)$ acquires an effective two-body part of the form

$$\begin{aligned} & \langle j^2 J_f \| T_{2\text{eff}}^{(\lambda)} \| j^2 J_i \rangle \\ &= \sqrt{2} (-)^{j+1/2+\lambda} \hat{j} \hat{\lambda} \hat{J}_i \hat{J}_f \sum_k \hat{j}_k \begin{pmatrix} j & \lambda & j_k \\ -\frac{1}{2} & 0 & \frac{1}{2} \end{pmatrix} I_{n\ell n_k \ell_k}^\lambda \\ & \times \sum_{J J'} \frac{\langle j^2 J | V_2 | j j k J \rangle}{\epsilon_j - \epsilon_{j_k}} \begin{Bmatrix} j & j_k & \lambda \\ J & J' & j \end{Bmatrix}, \end{aligned} \quad (1)$$

in terms of Wigner $3j$ and Racah $6j$ symbols [8,9], with $\hat{x} \equiv \sqrt{2x+1}$. The index k runs over the excluded orbits and J, J' take on the values $J_i J_f$ and $J_f J_i$. Furthermore, $I_{n\ell n_k \ell_k}^\lambda$ is a radial integral, and ϵ_{j_k} and $\langle j^2 J | V_2 | j j k J \rangle$ are single-particle energies and two-body interaction matrix elements, which in the following are taken from Ref. [12]. Once the two-body part of the effective transition operator is determined from Eq. (1), its matrix elements between many-nucleon states in the single- j shell can be obtained recursively [9]. This method therefore provides analytic, albeit approximate, expressions for the various properties calculated in the full shell-model space.

TABLE I. Energies in ^{134}Te and ^{135}I , calculated in perturbation theory of the first order (1) and of the second order with effective two- and three-body interactions ($2-V_2$ and $2-V_3$), compared with those obtained in the full space (Full).

Nucleus	J^π	Energy ^a (keV)				
		1	$2 V_2$	$2 V_3$	1 + 2	Full
^{134}Te	0^+	-738	-597		-1335	-1466
	2^+	-37	-65		-102	-130
	4^+	182	-28		154	145
	6^+	307	-12		295	290
^{135}I	$3/2^+$	405	-107	12	310	281
	$5/2_1^+$					-42
	$5/2_2^+$	268	-135	6	138	106
	$7/2^+$	-100	-508	14	-594	-755
	$9/2^+$	571	-83	12	500	484
	$11/2^+$	560	-89	6	478	453
	$15/2^+$	836	-46	-3	787	772

^aIn the single- j space the single-particle energy is set to zero; in the full space the single-particle energies are shifted such that $\epsilon_{g_{7/2}} = 0$.

Table I shows energies calculated in the various approximations. Following the nomenclature of Ref. [19], first-order perturbation theory corresponds to taking the matrix elements $\langle g_{7/2}^2; J | V_2 | g_{7/2}^2; J \rangle$ of the full space. It is seen that this leads to missing correlation energy, in particular in the paired states, $J^\pi = 0^+$ with seniority $\nu = 0$ in ^{134}Te and $J^\pi = 7/2^+$ with seniority $\nu = 1$ in ^{135}I . The effective interaction calculated to second order largely corrects for this, although some ~ 150 keV is still missing in the paired states. Two close-lying $J^\pi = 5/2^+$ levels are obtained in the full-space calculation for ^{135}I , with $5/2_2^+$ having the dominant $g_{7/2}^3$ configuration, which is therefore compared to the single- j state. Second-order perturbation theory gives rise to an effective interaction of two-body *and* three-body character. It is seen, however, that the latter effect is small, seldom exceeding 10% of the former.

Table II shows the $B(E2)$ values calculated with the one-body $E2$ operator or with an effective $E2$ operator with up to two-body terms, always with an effective charge of $e_\pi = 1.55e$. Agreement is found between the measured and calculated $B(E2; 15/2^+ \rightarrow 11/2^+)$ of ^{135}I when the full space is used. One notes that when up to two-body terms are used the resulting $B(E2)$ value depends in a delicate fashion on the phases of the different terms that enter Eq. (1). Nevertheless, it is seen that for most transitions the value calculated with an $E2$ operator with up to two-body terms in a single- j shell is closer to the full calculation. It is also seen that for some transitions the effect of the two-body terms can be important. This calls for caution in currently fashionable studies that include three-body

TABLE II. $B(E2)$ values in ^{134}Te and ^{135}I , calculated with an $E2$ operator with a one-body term (1) or with up to two-body terms (1 + 2), compared with those obtained in the full space (Full) and with the measured values (Exp).

Nucleus	J_i^π	J_f^π	$B(E2; J_i^\pi \rightarrow J_f^\pi)$ (W.u.)			
			1	1 + 2	Full	Exp
^{134}Te	2^+	0^+	3.78	4.25	4.27	5.08(20)
	4^+	2^+	3.78	4.08	4.27	4.30(39)
	6^+	4^+	1.72	1.77	1.89	2.04(5)
^{135}I	$11/2^+$	$7/2^+$	4.18	4.72	4.47	
	$15/2^+$	$11/2^+$	3.08	3.40	3.67	3.81(17)
	$5/2_1^+$	$7/2^+$			0.083	
	$5/2_2^+$	$7/2^+$	9.21	10.40	9.72	
	$9/2^+$	$7/2^+$	1.56	1.77	1.77	
	$9/2^+$	$11/2^+$	3.21	2.63	2.29	

terms in the Hamiltonian but neglect a consistent treatment of effective transition operators.

The half-life of the $15/2^+$ state of the 3-valence-proton nucleus ^{135}I was measured using a direct-timing method. The nuclei of interest were populated following the cold neutron-induced fission of a thick ^{235}U target at the PF1B facility of the ILL. Prompt γ rays emitted by secondary fission fragments were measured using a mixed array of Ge and LaBr₃ detectors and the timing signals between the latter detectors used to extract a half-life of $T_{1/2} = 1.74(8)$ ns for the $15/2^+$ state of ^{135}I . This measurement enabled for the first time a test of seniority relations between $B(E2)$ values in neighboring nuclei. Large-scale shell-model calculations were performed for ^{134}Te and ^{135}I , and reinterpreted in a single-orbit $g_{7/2}$ approach, leading to the conclusion that energy shifts due to the three-body component of the effective interaction are small and that the effect of the two-body component of the $E2$ operator can be large.

This work was supported by NuPNET and the German BMBF by Contracts No. 05P12PKNUF and No. 05P12DRNUP; the Spanish MINECO via Projects No. FPA2015-65035-P, No. CPAN (CSD 2007-00042), and No. PRI-PIMNUP-2011-1338 within the ERA-NET NuPNET call for translational joint activities; and the UK STFC by Contract No. DNC7RP01/4 and the UK National Measurement Office. The EXILL-FATIMA campaign would not have been possible without the support of several services at the ILL and the LPSC. We are grateful to the EXOGAM collaboration for the loan of the detectors, to GANIL for assistance during installation and dismantling, and to the FATIMA collaboration for the provision of LaBr₃(Ce) detectors and analog electronics.

- [1] E. Caurier, G. Martínez-Pinedo, F. Nowacki, A. Poves, and A. P. Zuker, *Rev. Mod. Phys.* **77**, 427 (2005).
 [2] H.-W. Hammer, A. Nogga, and A. Schwenk, *Rev. Mod. Phys.* **85**, 197 (2013).
 [3] J. Sinatkas, L. D. Skouras, D. Strottman, and J. D. Vergados, *J. Phys. G: Nucl. Part. Phys.* **18**, 1377 (1992).

- [4] L. Coraggio, A. Covello, A. Gargano, and N. Itaco, *Phys. Rev. C* **80**, 044311 (2009).
 [5] M. Nomura, *Phys. Lett. B* **40**, 522 (1972).
 [6] A. Frank, J. Jolie, and P. Van Isacker, *Symmetries in Atomic Nuclei: From Isospin to Supersymmetry* (Springer, New York, 2009).

- [7] G. Racah, *Phys. Rev.* **63**, 367 (1943).
- [8] A. Shalit and I. Talmi, *Nuclear Shell Theory*, Pure and Applied Physics (Academic Press, New York, 1963).
- [9] I. Talmi, *Simple Models of Complex Nuclei* (Harwood Academic, Chur, Switzerland, 1993).
- [10] J. P. Omtvedt, H. Mach, B. Fogelberg, D. Jerrestam, M. Hellström, L. Spanier, K. I. Erokhina, and V. I. Isakov, *Phys. Rev. Lett.* **75**, 3090 (1995).
- [11] C. T. Zhang, P. Bhattacharyya, P. J. Daly, R. Broda, Z. W. Grabowski, D. Nisius, I. Ahmad, T. Ishii, M. P. Carpenter, L. R. Morss, W. R. Phillips, J. L. Durell, M. J. Leddy, A. G. Smith, W. Urban, B. J. Varley, N. Schulz, E. Lubkiewicz, M. Bentaleb, and J. Blomqvist, *Phys. Rev. Lett.* **77**, 3743 (1996).
- [12] C. Goodin, N. J. Stone, A. V. Ramayya, A. V. Daniel, J. R. Stone, J. H. Hamilton, K. Li, J. K. Hwang, Y. X. Luo, J. O. Rasmussen, A. Gargano, A. Covello, and G. M. Ter-Akopian, *Phys. Rev. C* **78**, 044331 (2008).
- [13] M. Samri, G. J. Costa, G. Klotz, D. Magnac, R. Seltz, and J. P. Zirnheld, *Z. Phys. A* **321**, 255 (1985).
- [14] H. Abele, D. Dubbers, H. Häse, M. Klein, A. Knopfler, M. Kreuz, T. Lauer, B. Markisch, D. Mund, V. Nesvizhevsky, A. Petoukhov, C. Schmidt, M. Schumann, and T. Soldner, *Nucl. Instrum. Methods Phys. Res. A* **562**, 407 (2006).
- [15] J.-M. Régis, G. Simpson, A. Blanc, G. de France, M. Jentschel, U. Koester, P. Mutti, V. Pazyi, N. Saed-Samii, T. Soldner, C. Ur, W. Urban, A. Bruce, F. Drouet, L. Fraile, S. Ilieva, J. Jolie, W. Korten, T. Kroll, S. Lalkovski, H. Mach, N. Marginean, G. Pascovici, Z. Podolyak, P. Regan, O. Roberts, J. Smith, C. Townsley, A. Vancraeynest, and N. Warr, *Nucl. Instrum. Methods Phys. Res. A* **763**, 210 (2014).
- [16] W. Urban, M. Jentschel, B. Markisch, T. Materna, C. Bernards, C. Drescher, C. Fransen, J. Jolie, U. Koester, P. Mutti, T. Rząca-Urban, and G. Simpson, *J. Instrum.* **8**, P03014 (2013).
- [17] A. Poves and A. Zuker, *Phys. Rep.* **70**, 235 (1981).
- [18] A. Volya, *Europhys. Lett.* **86**, 52001 (2009).
- [19] P. Van Isacker and I. Talmi, *Europhys. Lett.* **90**, 32001 (2010).